Science of Sintering, **41** (2009) 161-173

doi: 10.2298/SOS0902161F

UDK 622.785:621.762

Bonding Evolution with Sintering Temperature in Low Alloyed Steels with Chromium

L. Fuentes-Pacheco[1*)], M. Campos[1,2]
Universidad Carlos III de Madrid
[1]Materials Science and Engineering Department,
[2]IAAB, Avda de la Universidad 30. 28911, Leganés (Madrid). Spain

Abstract:

At present, high performance PM steels for automotive applications follow a processing route that comprises die compaction of water-atomized powder, followed by sintering and secondary treatments, and finishing operations. This study examines Cr-alloyed sintered steels with two level of alloying. In chromium-alloyed steels, the surface oxide on the powder is of critical importance for developing the bonding between the particles during sintering. Reduction of this oxide depends mainly on three factors: temperature, dew point of the atmosphere, and carbothermic reduction provided by the added graphite. The transformation of the initial surface oxide evolves sequence as temperature increases during sintering, depending on the oxide composition. Carbothermic reduction is supposed to be the controlling mechanism, even when sintering in hydrogen-containing atmospheres. The effect of carbothermic reduction can be monitored by investigating the behavior of the specimens under tensile testing, and studying the resultant fracture surfaces.

Keywords: *Sintered steels, Chromium, Sintering contacts, Mechanical properties.*

1. Introduction

The final properties of materials made from powders depend upon the strength of the bonding between the particles, and on the amount, shape, and distribution of porosity. The oxide layer that exists at the surface of all metal powders hinders mass transports and inhibits diffusion between particles. The stability of this oxide layer depends on the composition of the metal powder.

Chromium and molybdenum are widely used as alloying elements in conventional ingot steels. Both elements are carbide formers and alpha phase stabilizers, and both greatly improve the hardenability of steels [1]. Due to the solid solution hardening effect, Cr and Mo enhance tensile and yield strength as well as hardness. Molybdenum also advances the rate of the bainitic transformation, affording the opportunity to obtain bainitic steels with high toughness over a wide range of cooling rates. The addition of Mo can compensate for the low ductility produced by high tempering temperatures, decreasing the commonly resulting brittleness. Additional advantages of chromium as an alloying element include low price and easy recyclability. As a result of these benefits, low alloyed Cr-Mo steels are used when parts require hardenability, high tensile strength, and good wear behavior. However, the higher

*) Corresponding author: mfuentes@ing.uc3m.es

sensitivity of chromium to oxidation during sintering, even in a prealloyed state, represents the main limitation for producing PM parts from this alloying system [2, 3, 4].

This paper explores the effects of composition and processing conditions on the developed microstructure, sintering bonding, and hence, the material behavior of such alloys.

Experimental procedure

To study the influence of the alloying elements on the sintering progress, three compositions with different oxygen affinity were chosen. All of these alloy compositions were produced by Höganäs AB (Sweden), using a standard water atomization process with subsequent annealing (see Tab. I). The first composition was a water atomized Fe powder, which was the reference material because of its low oxygen affinity. The other two compositions were prealloyed Fe powders with different Cr and Mo contents.

Tab. I. Nominal chemical compositions of the studied powders

Material	Nomenclature	O-tot, %	Chromium	Molybdenum	Iron
Fe powder	ASC	0.08	-	-	100
Low Cr alloyed	CrL	0.16	1.50	0.20	Bal.
High Cr alloyed	CrM	0.21	3.00	0.50	Bal.

Mixtures with 0.6 wt.% graphite were processed in a turbula-type spatial blender for 40 min. After blending, tensile bars were compacted at 700 MPa in a uniaxial press with wall lubrication of the die, then sintered in a lab tubular furnace under a $90N_2$-$10H_2$-CH_4 atmosphere at a sintering pressure just above 1 atm, with a heating and cooling rate of 5ºC/min and a holding time of 30 minutes. The sintering atmosphere provides a reducing agent (H_2) that, together with graphite additions, prevents the oxidation of chromium at temperatures higher than 980ºC [5], minimizing the risk of carbon loss. To assess the evolution of the oxide layer reduction, i.e., the bonding between particles, and the diffusion of carbon, the samples were sintered from 600ºC to 1200ºC in increments of 100ºC.

Sintered samples were characterized by chemical analysis, microstructural analysis, and mechanical testing. Oxygen and carbon content were measured with a LECO TC500 and CS200. Microstructural analysis was performed following standard metallographic procedures. Mechanical properties were measured by means of tensile tests and Vickers hardness tests. Fracture surface analysis was also performed to show the features of bonding as the sintering temperature was increased. Investigations regarding the combined carbon content, mechanical response, and neck characteristics demonstrate the effectiveness of the present reducing agents at high temperatures.

The study of porosity in this system (by image analysis) and density (by the method of Archimedes) with sintering temperature helped to explain the observed behavior of the sintered materials. Pore features were determined using three different parameters: pore area (μm^2), f_{circle}, and f_{shape} (f_c, and f_s, respectively) over unetched specimens [6].

Results and Discussion

In prealloyed powders with chromium, the heterogeneous surface oxide has a mixed cation composition (from Fe and Cr) and a thickness between 6 to 10 nm [7, 8].

The presence of this layer surrounding the particles inhibits the diffusion processes

that take place during sintering. However, the mixed composition of this oxide enables the use of sintering atmospheres with a higher P_{O2} than would be calculated from the Ellingham diagram, due to the formation of Cr_2O_3 (approx~ $5 \cdot 10^{-18}$ atm as reported in [9, 10]).

Several works have examined the effect of agents that promote reduction of this layer. Considering the composition of the sintering atmosphere and the proposed alloying systems for this study, and considering N_2 as an inert gas, the most relevant reduction reactions [11, 12, 13] that can occur are:

$MO+H_2 \leftrightarrow M+H_2O$	Reduction by H_2	(1)
$MO+C \leftrightarrow M+CO$	Direct carbothermal reaction	(2)
$C + CO_2 \leftrightarrow 2CO$	Boudouard's reaction	(3)
$MO+CO \leftrightarrow M+ CO_2$	Reduction by CO/CO_2	(4)

It is necessary to consider that, depending on the reaction, reduction can start from the surface of the components (H_2) or in the internal pores (C). The H_2 present in the atmosphere governs the reduction at relatively low temperatures, in the range of 1000º to 1100º C, for chromium systems. At higher temperatures, the activity of carbon in the austenite and the ratio of CO/CO_2 are the agents responsible of further reduction. In this case, we can assume that the ratio CO/CO_2 for chromium-containing steels will be similar in all the sintering processes.

The products of the proposed reactions can displace the previous atmosphere, modifying the concentration of reducing agents with temperature. This modification could, in turn, affect the success of inter-particle bond development. This work explores the sequence of bond formation depending on powder composition and sintering temperature. To determine the consequences of temperature changes, we study the evolution of porosity and the concentration of oxygen and carbon. We also examine the fracture surfaces just after tensile testing.

Influence of sintering temperature on oxygen and combined carbon contents

The variation of oxygen and carbon content with sintering temperature is shown in Fig. 1. The Fe-C system shows large oxygen losses around 700ºC and 1000ºC that, according to [14], correspond to the reduction of surface and internal oxides, respectively. The evolution of combined carbon content runs parallel to oxygen losses, which confirms that carbon acts as the main reducing agent of iron oxides.

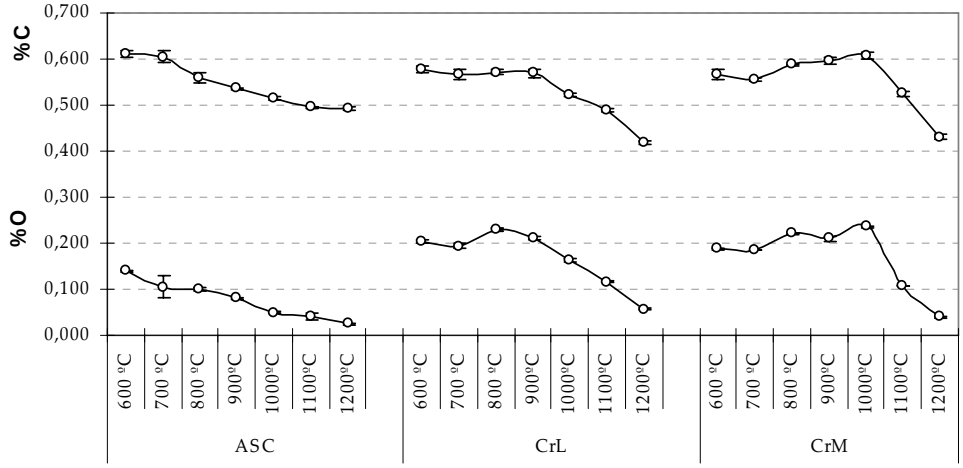

Fig. 1. Oxygen and carbon evolution with sintering temperature

Comparing the three alloying systems, some differences are clear. In chromium-alloyed steels, oxidation starts at 800ºC. In the case of high-alloyed chromium steel, this oxygen gain remains until 1000ºC. At the same time, carbon content does not decrease. These facts can be taken as a sign that the currently investigated atmospheric composition is inappropriate for sintering of these materials in that temperature range.

Past 1000ºC, the oxygen content decreases due to the reduction provided by the carbon diluted in the austenite, and the CO/CO_2 ratio in the atmosphere. The high Cr-alloyed steels do not undergo the reductions described in reactions (2) and (4) until 1100ºC. The carbon loss of these specimens depends on the amount of chromium, which is directly related to the presence of a higher concentration of chromium cations (Cr^{3+}) in the oxide layer. The presence of this higher concentration of cations leads to a higher stability. Therefore, to achieve reduction at the given CO/CO_2 ratio, the high-alloyed chromium steel requires higher temperatures than do the reference and low-alloyed Cr steels. The complete removal of oxides is only achieved when sintering is performed up to 1200ºC. Moreover, the oxygen content after sintering up to 1200ºC is the same for all samples, which means that the surface layer and internal oxides were removed.

Bonding evolution with sintering temperature

There are some tests that can reveal the extent of bonding at different sintering temperatures. Metallographic examination, coupled with image analysis, and density measurements can provide information about the pore evolution and the length of necks between particles.

Below a sintering temperature of 800ºC, there are no differences in contact length for any of the studied materials. No contacts are formed, the initial particles are still visible, and there is no carbon diffusion. Graphite is retained around the ferrous particles, and the microstructure is ferritic.

Images of the Fe-C system at 800ºC in Tab. II show the formation of incipient sintering necks and the presence of some pearlite grains. These phenomena prove that carbon diffusion has begun. According to Fig. 1, at 900ºC, the surface oxide has been totally reduced and diffusion processes are favored. At 1000ºC, the sintering process and the diffusion of carbon seem complete. We observed no significant difference between the samples sintered at 1100ºC and those sintered at 1200ºC.

For low-alloyed chromium steel, the microstructure does not evolve until 900ºC. At this temperature, large zones of pearlite appear in the ferritic microstructure, but there is no evidence of contact formation. It seems that the presence of surface oxides restricts the auto-diffusion processes (which lead to contact formation and neck growth) to a greater extent than does carbon dissolution. Carbon diffusion is not complete until 1000-1100ºC. There are apparently contacts between particles at 1000ºC, although it is difficult to observe these contacts with optical microscopy. This hypothesis must be confirmed with fractography observations.

The evolution of high-alloyed steels is similar to that of steels with lower chromium content, but delayed at higher temperatures. This delay is in accord with the evolution of oxygen content (Fig. 1). Pearlite formation starts at 1000ºC, which demonstrates the beginning of the carbon diffusion, but the edges of the initial particles are still visible. Contact formation is clear at 1100ºC, and carbon diffusion is finished at 1200ºC, which results in a fully pearlitic microstructure. The pearlite is thinner and more abundant in the Cr-Mo containing steels, due to the displacement of the CCT curves caused by the alloying element content.

Quantity, interconnection, size and morphology are the main features of pores that can modify the final material properties. In this case, we evaluated the effect of sintering

temperature on quantity, size and morphology of porosity in terms of cumulative and frequency distributions (Fig. 2 and Fig. 3).

Tab. II. Sequence of microstructures with sintering temperature of the studied systems. The low cooling rate leads to ferritic-pearlitic microstructures.

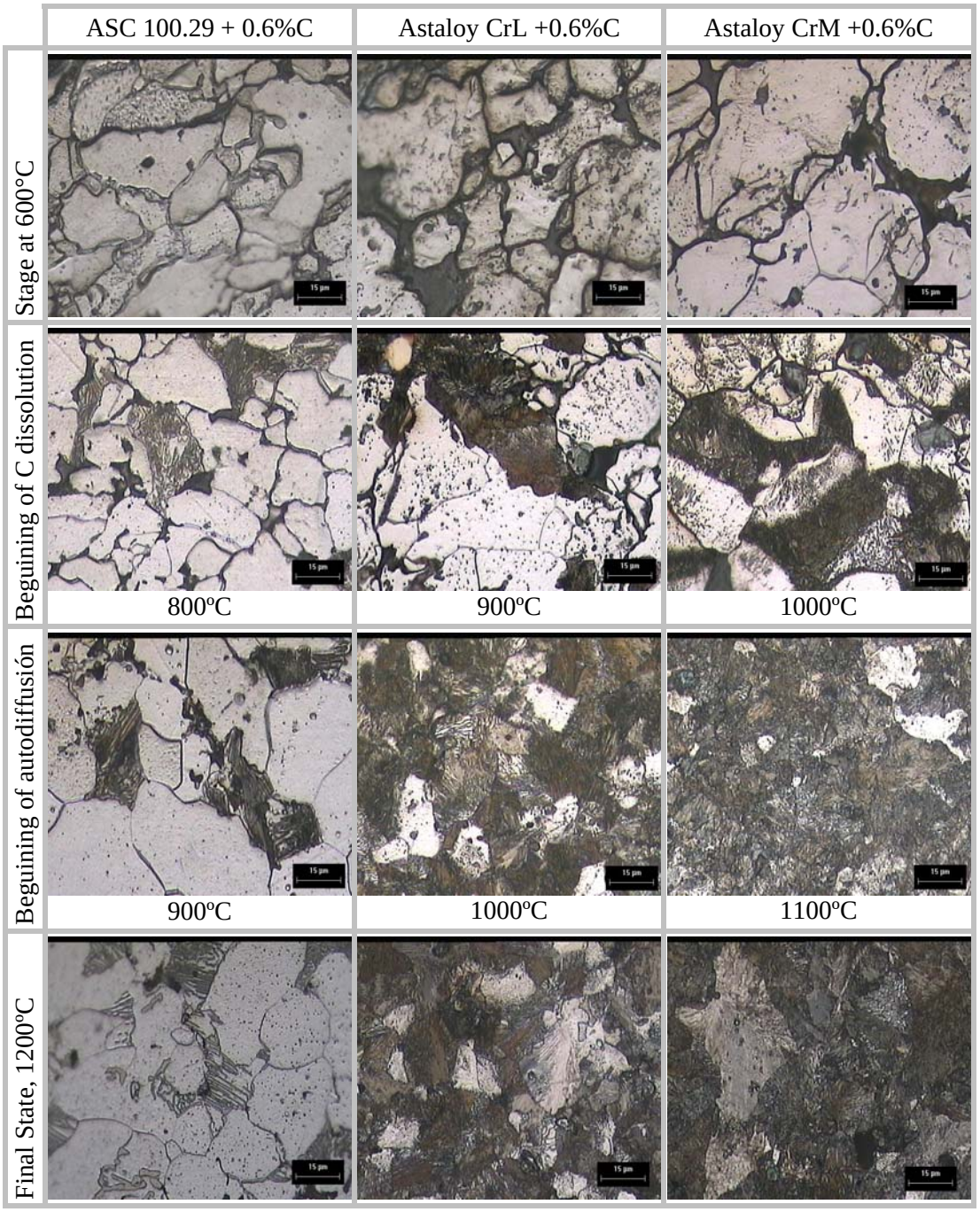

After the initial particle bonding, as sintering temperature is increased, there are different stages that bonding powders experience: neck growth, reduction of pore interconnection and shrinkage (densification), pore rounding, and pore coarsening (normally

only at high sintering temperatures or long sintering times). All of these stages are related to mass transport phenomena that take place in the sintering cycle.

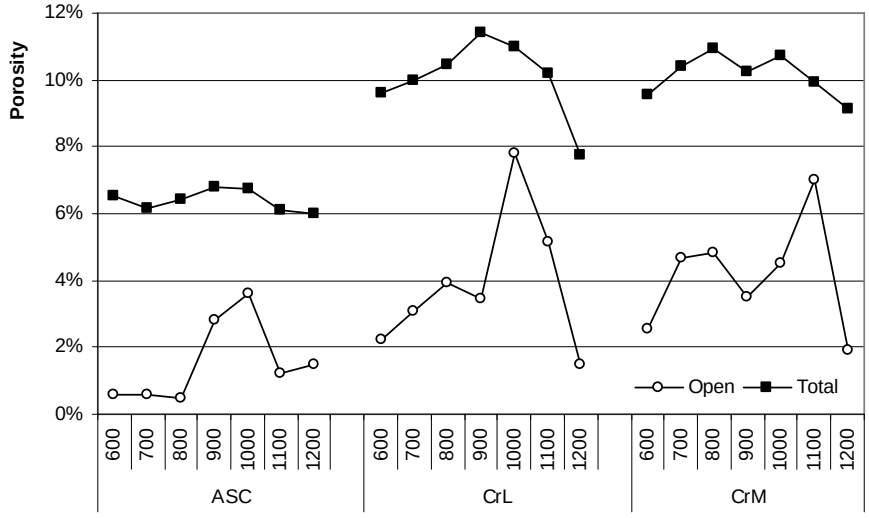

Fig. 2. Total and open porosity with sintering temperature.

Fig. 2 shows the evolution of total and open porosity values of the three materials with sintering temperature. The total porosity of the reference material is lower at all temperatures due to the lower compressibility of chromium prealloyed powders, which leads to a lower green density of the compacts. The total porosity of all the materials evolves in the same way as does the oxygen content. That behavior confirms that contacts begin to form and pores shrink only when the oxide layer of the particles is reduced. Based on the open porosity values, it seems that the gases produced in the reduction reaction open the pores on their way out. Once the reaction gases have been incorporated to the atmosphere, the pores close as the sintering process occurs.

After initial stage of sintering, in which neck formation takes place, mass transports mechanisms leads to changes in the structure of pores. In a second stage, diffusion processes produce pore shrink and, as a consequence, a decrease in the dimensions of the compact. After this stage, the sintered body still contains a wide rage of pore sizes and shapes. The late sintering stage is characterized by changes in the structure and the nature of pores: pore size distribution becomes narrower and pore surface becomes softer and round.

Studying size distribution and shape parameters of the porosity of the samples sintered at different temperatures (Fig. 3) allows determination of the stage of sintering and the delay that the presence of stable oxide layers produces in the diffusion mechanisms.

In order to study the evolution of pore size, we plotted the cumulative frequency of pore area in Fig. 3, left. As expected, the percentage of pores of smaller size increases with sintering temperature, exhibited as a displacement of the curves to the right. The evolution of the pore size of Fe-C and low-alloyed Fe-Cr-Mo-C systems is similar. It is important to note the large area reduction present between 1000ºC and 1200ºC. This fact, together with the rounding of the pores, will have a significant influence in properties like ductility. In the high-alloyed Fe-Cr-Mo-C system, the process of pore shrinkage is delayed due to the higher stability of the surface oxides. From the graphs, we can conclude that the size distribution of the pore system of this alloy after sintering at 1200ºC is equivalent to the distribution of the other two materials sintered at 1000ºC.

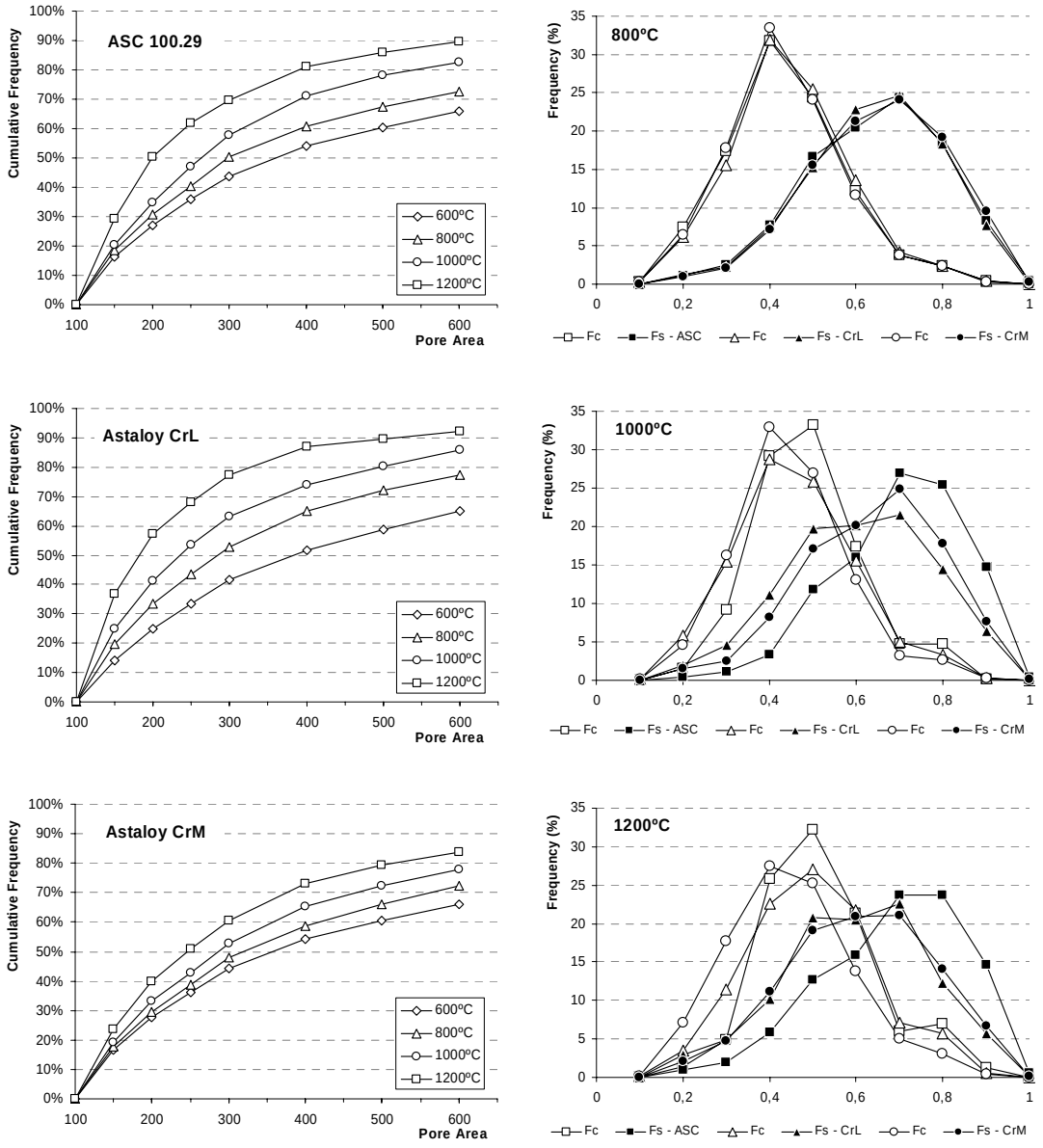

Fig. 3. Characteristics of porosity with sintering temperature depending on the studied steel. Left: area of pores (μm^2) and right: shape parameters (fcircle -white spot- and fshape –full spot-).

We examined the morphology of the porosity in terms of the shape parameters f_{shape}, and f_{circle}, which quantify the elongation and the irregularity of the pores, respectively. Values close to 1 reveal a round and regular porosity. Other studies have found that high sintering temperatures improve the f_{circle} parameter more than f_{shape} [6, 15]. This phenomenon is a consequence of the fact that irregularities in the surface have a smaller radius of curvature than does the pore itself. This higher curvature leads to a larger driving force for the mass transport mechanisms.

At the lower sintering temperature, f_{circle} has a distribution centered around 0.4 for the three materials. In the Fe-C system, the distribution is shifted to higher values when the sintering temperature is increased. This tendency is also followed, to a lesser extent, by the low chromium-alloyed steel, whereas the distribution hardly evolves for the studied

temperatures in the case of high chromium-containing steel. Only the Fe-C system shows a marked evolution of f_{shape} at the studied sintering temperatures. In this system, f_{shape} increased with increasing temperature. The chromium-containing materials show a slight increase in porosity, with values of f_{shape} greater than 0.5. As pore rounding is connected to final stages of sintering, only the Fe-C system has achieved that point at 1000-1200ºC. The other two materials do not seem to evolve in this sense. Therefore, by studying the shape parameters of the porosity, it is possible to detect the presence of a stable oxide coating the particle, which delays the progression of sintering.

The measured density of the as-sintered specimens is shown in Fig. 4. The density of the Fe-C samples is higher than the values obtained for Cr-containing materials. The larger compressibility of Fe powder makes the green density of the compacts higher, so higher values of final density can be achieved.

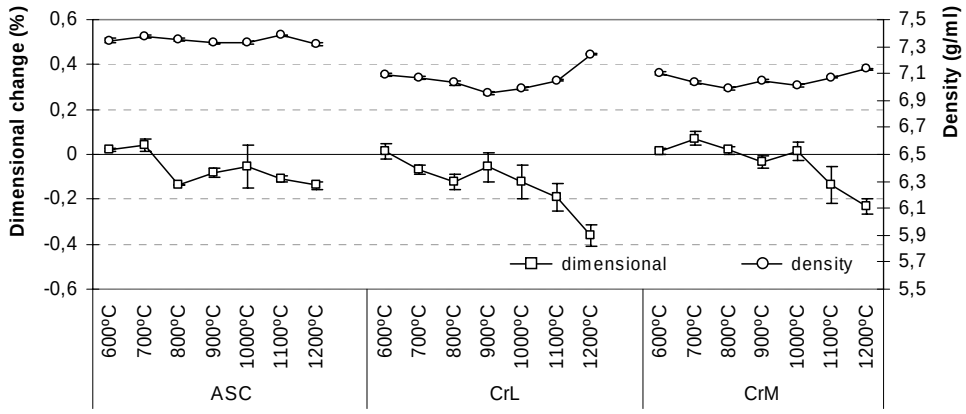

Fig. 4. Evolution of density and dimensional changes with the sintering temperature.

The density of the specimens shows a dependence on oxygen content. The samples undergo swelling when oxidation takes place, and contraction when the oxides are reduced and the sintering process begins. Once the oxides are eliminated, an increase of density with sintering temperature is expected. As was stated before, the densification can be understood in terms of pore shrinkage, and depends on the amount of pores in the green specimens. For this reason, higher compressibility results in higher green density and, consequently, less densification of the compact during sintering. This relationship is the reason for the larger densification exhibited by the low-alloyed chromium steel in comparison to the reference material. In the high chromium steel, we observed an increasing trend of density after sintering over 1000ºC, and expect a greater extent of densification for sintering temperatures higher than 1200ºC.

The dimensional change of the specimens is consistent with the density measurements. The samples swell at the sintering temperatures at which oxidation is induced, and shrink when the contacts among the particles grow and close the porosity (see Fig. 4). As was expected, the chromium-containing steels underwent a larger shrinkage due to their lower green density.

Mechanical properties

In porous materials, the hardness depends not only on the resistance of the material to penetration by the indenter, but also on the strength of the contacts established among the particles, and on the amount of porosity.

In the Fe-C system (Tab. III), a moderate increase in hardness is produced between 700ºC and 1000ºC. The apparent hardness is a consequence of the presence of carbon in the microstructure, the bonding among the particles, and the porosity. Taking this in to consideration, the diffusion processes in this case seem to begin at 700-800ºC and finish at 1000ºC, because from there on, the hardness values stay constant.

Tab. III. Mechanical properties of the as-sintered specimens. Hardness, ultimate tensile stress, yield stress, Young's modulus and fracture strain are shown. The brittleness of some samples sintered at low temperatures only allowed determination of the UTS and strain values.

	Fe-C					CrL					CrM				
T ºC	UTS (MPa)	YS (MPa)	%ε	E (GPa)	HV30	UTS (MPa)	YS (MPa)	%ε	E (GPa)	HV30	UTS (MPa)	YS (MPa)	%ε	E (GPa)	HV30
600	14 ± 1	-	0,11 ± 0.02	-	93 ± 6	7 ± 1	4 ± 1	0,43 ± 0.19	-	95 ± 8	4 ± 0	-	0,20 ± 0.04	-	93 ± 5
700	21 ± 18	15 ± 13	2,57 ± 0.27	-	67 ± 4	12 ± 3	6 ± 3	0,29 ± 0.11	-	83 ± 6	5 ± 0	-	0,27 ± 0.08	-	66 ± 4
800	160 ± 6	104 ± 4	3,61 ± 0.77	69 ± 13	67 ± 2	19 ± 3	6 ± 1	0,24 ± 0.20	-	71 ± 3	10 ± 1	7 ± 1	0,12 ± 0.04	-	78 ± 2
900	218 ± 5	134 ± 2	4,94 ± 0.52	77 ± 9	80 ± 5	50 ± 24	32 ± 8	0,20 ± 0.04	24 ± 9	84 ± 1	27 ± 12	20 ± 8	0,22 ± 0.04	36 ± 9	80 ± 4
1000	258 ± 6	161 ± 8	4,90 ± 0.12	92 ± 32	97 ± 2	312 ± 14	207 ± 34	1,54 ± 0.72	119 ± 22	136 ± 7	196 ± 8	164 ± 1	0,50 ± 0.03	59 ± 10	94 ± 6
1100	298 ± 9	182 ± 4	7,17 ± 0.34	99 ± 4	97 ± 7	449 ± 8	266 ± 10	2,75 ± 0.29	127 ± 32	171 ± 5	555 ± 8	412 ± 9	1,48 ± 0.19	102 ± 13	200 ± 6
1200	326± 19	203 ± 17	7,68 ± 1.33	108 ± 21	101 ± 2	468 ± 18	272 ± 12	4,39 ± 0.66	149 ± 15	146 ± 7	629 ± 15	423 ± 3	2,14 ± 0.24	123 ± 7	220 ± 12

The presence of Cr and Mo in solid solution enhances hardness, given the presence of carbon. That enhancement explains why the apparent hardness of the chromium-containing steels only increases when carbon diffusion begins. The evolution of apparent hardness with sintering temperature of the studied samples shows that carbon diffusion in low-alloyed chromium steel begins at 800ºC, and finishes at 1100ºC. In high-alloyed chromium steel, the dissolution of carbon starts at temperatures higher than 1000ºC. The comparison between the three materials underlines the influence of chromium on the hardness of steel. It has to be taken into account that the carbon content of both chromium steels is lower due to the carbothermic reduction processes. The difference in hardness would likely be greater if the carbon content of all the compositions was the same. The influence of chromium and molybdenum on hardness would also be even more important after a thermal treatment that led to a harder microstructure.

We calculated the values of ultimate tensile strength, yield strength, Young's modulus, and strain at break from the stress-strain curves. However, due to the brittleness of some samples sintered at low temperatures, we were only able to obtain the UTS and the strain values for those samples.

The UTS of sintered steels depends on composition, density, porosity, heat treatment, and process conditions [16, 17]. In our case, this means that acceptable values of UTS will be achieved when the interparticle contacts are large and strong, which it is connected with a stage at the sintering process that lead to small, rounded, and uniformly distributed pores. On the other hand, carbon diffusion will enhance the UTS due to solid solution strengthening (see Fig. 5).

In case of Fe-C, the experimental measurement of tensile properties suggests that carbon diffusion, growth of sintering necks, and the roundness of pores are important. Evolution of these features begins at 800ºC and seems to be complete at 1000ºC. In the chromium-containing steels, these processes are delayed. For low-alloyed chromium steels, the change in UTS appears at 1000ºC, and seems complete at 1100ºC. In high-alloyed steels, UTS does not significantly change until 1100ºC, and the change is not complete at 1200ºC. The values of UTS are proportional to the content of alloying elements. Yield strength and Young's modulus values agree with the UTS values. Young's modulus is very sensitive to the shape and size of porosity, so the presence of irregular pores considerably decreases its value. That relationship is why the moduli of the low-alloyed chromium materials are larger than those of high-chromium alloys.

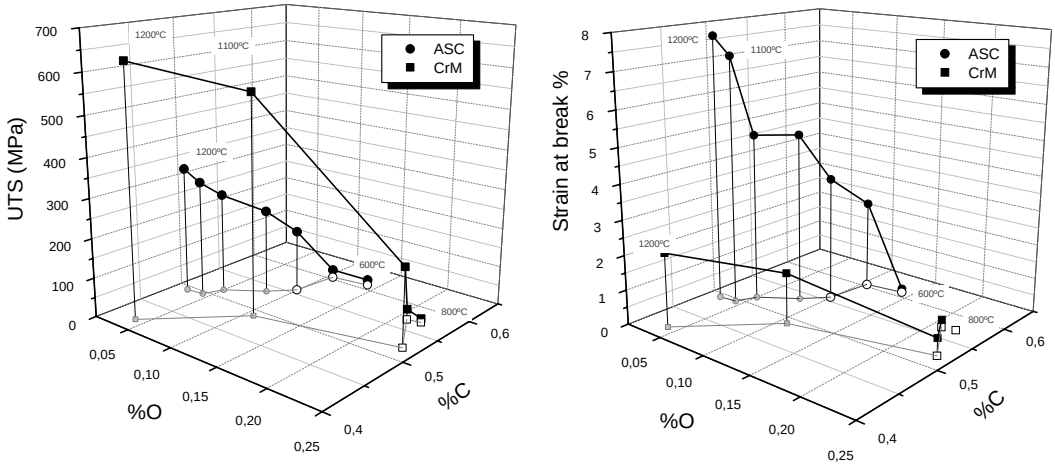

Fig. 5 Relationship between UTS and strain at break and final oxygen and carbon content as the sintering temperature is increased. In the %O - %C plane, the filled points indicate that carbon is totally combined, whereas the empty points indicate the presence of free graphite in the microstructure.

The fracture strain data show the influence of alloying elements. Chromium and molybdenum in solid solution hinder the movement of dislocations, decreasing the ductility of the material. However, the most remarkable aspect is the influence of contact quality and pore geometry on the mechanical properties.

At the highest sintering temperatures, the values of hardness and UTS are barely enhanced, whereas fracture strain is clearly increased. Lower temperature sintering is sufficient to form strong contacts and dissolve carbon, but the increase of temperature leads to rounded pores, which provide larger ductility by decreasing the notch effect. This increase of ductility with sintering temperature is particularly prominent in the Fe-C and low Fe-Cr-Mo-C systems. In the high-Cr steel, we expect ductility to be larger if the sintering temperature is higher than 1200ºC (i.e. 1250ºC), because of the delay in the sintering process.

Fractography

We analyzed the fracture surfaces by SEM to determine the main fracture micromechanisms, as well as the growth and quality of sintering necks (Tab. IV).

The fracture surfaces of all specimens sintered at 600ºC and 700ºC are similar: there is no evidence of strong contacts between the particles, as all surfaces remain intact. The only difference between the samples is the larger deformation of plain Fe particles (ASC), due to

the higher compressibility of this powder.

Tab. IV. Fracture surface analysis.

	ASC 100.29 + 0.6%C	Astaloy CrL +0.6%C	Astaloy CrM +0.6%C
900°C	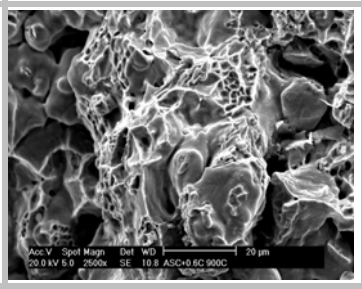	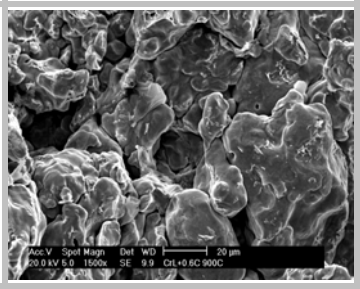	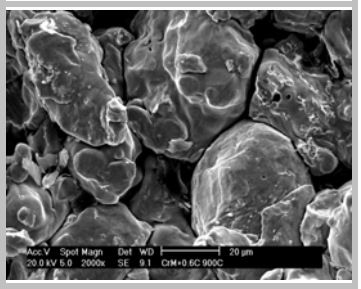
1100°C	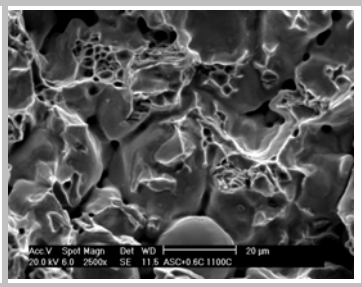	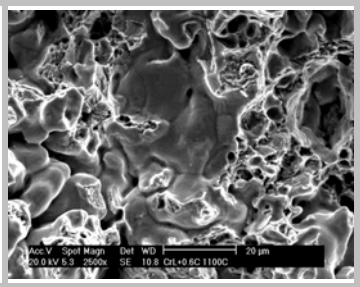	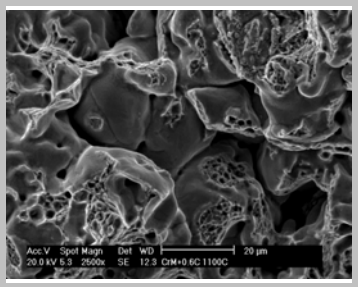
1200°C	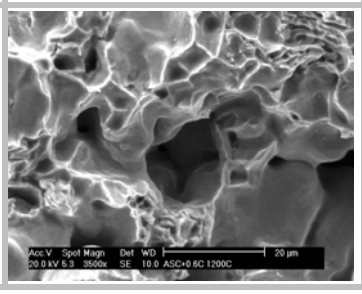	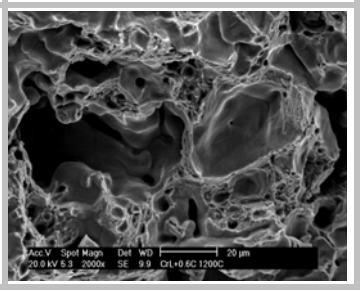	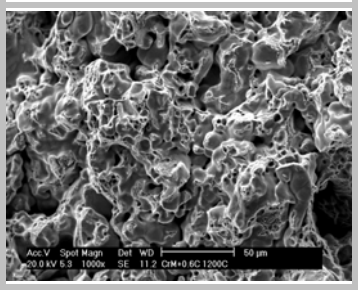

From 800ºC on, the evolution of the materials changes. In the Fe-C system at 800ºC, there are small necks torn by microvoid coalescence, typical of a ductile fracture, but these are not widespread until 900ºC. At higher temperatures, necks are more deformed and deformation edges can be seen all over the fracture surface. There is no evidence of cleavage or decohesion planes, so the dominant fracture micromechanism is, therefore, ductile fracture of sintering necks. This result means that the necks are strong enough to deform prior to fracture, but that they are not able to transmit the load to the particles.

In low-alloyed chromium steel, the first broken necks appear at 1000ºC, but the initial particles are visible until 1200ºC. At this temperature, necks seem well-formed and there is more deformation around them. Again, the main fracture micromechanism is ductile fracture of sintering necks due to microvoid coalescence, although, in this case, there are no deformation edges in the fracture surface.

In high-alloyed chromium steel, some necks appear broken by microvoid coalescence at 1100ºC, but the initial particles are still visible and the contact area is small. At 1200ºC, necks have grown and microvoids are evident all over the fracture surface, but some boundaries of the initial particles can still be distinguished, and porosity is still noticeable. The general morphology of the fracture surface of this steel sintered at 1200ºC is similar to that of the low chromium-containing steel sintered at 1100ºC, or by the reference sample sintered at 1000ºC.

Conclusions

Based on the cited results, we can draw several conclusions:

- The presence of elements with high oxygen affinity (like chromium) enhances the stability of the surface oxide layer. The sintering process therefore requires a higher sintering temperature and tight control of the atmosphere.
- As a result of the higher stability of the oxides that contain chromium, oxygen losses occur at higher temperatures. Chromium steels also show oxidation at low sintering temperatures (around 800º-900ºC). Carbon is the main reducing agent at high temperatures, and the carbon loss has to be taken into account in the initial composition.
- Diffusion processes do not begin until the surface oxides are reduced. Carbon diffusion takes place before than the formation and growth of the sintering necks. The evolution of the quantity density of pores with sintering temperature shows a decrease when necks between particles start to form. Studying the open porosity allows determination of when the reduction of surface oxides takes place, as open porosity increases at that time.
- Analyzing the shape parameters of the pore morphology allows detection of the presence of a stable oxide coating the particle. This coating delays the stages of sintering.
- Despite the fact that the final microstructures are ferritic/pearlitic due to the low cooling rate, reasonable mechanical properties can be obtained after sintering low-alloyed chromium steels at 1120ºC in a proper atmosphere. However, temperatures over 1200ºC are necessary to obtain optimum results.

In general, the whole sintering process is delayed due to the presence of chromium. This effect becomes greater as the chromium content increases.

Acknowledgements

The authors gratefully acknowledge financial support from the Comunidad de Madrid to carry out this investigation through the program ESTRUMAT-CM (reference MAT/77) and CICYT through the R&D project MAT2006-02458.

References

1. ASM Handbook, “Powder Metal Technologies and Applications”, Vol. 7, ASM International, Material Park, OH, 1998
2. L. Arnberg, A. Karlsson, Int. J. Powder Metall., 24 (1988) 107.
3. S.Kremel, H.Danninger, Y.Yu. Powder Metall., Progress 2 (2002) 211.
4. M. Campos, L. Blanco, J. Sicre-Artalejo, JM. Torralba, Rev. Metal. Madrid., 44 (2008) 5.
5. H. Danninger, C. Gierl. Sci. Sinter., 40 (2008) 33.
6. T. Marcu Puscas, M. Signorini, A. Molinari, G. Straffelini. Mater. Charact., 50 (2003) 1–10
7. H. Karlsson, L. Nyborg, S. Berg. Powder Metall., 48 (2005) 51.
8. P. Ortíz, F. Castro, Powder Metall., 47 (2004) 291.
9. C. Lindberg, in Proc. PM2TEC’99, Vancouver, Canada, 1999.
10. H. Danninger, C. Gierl. Mater. Chem. Phys., 67 (2001) 49.

11. A. Cias, S.C Mitchell, K. Pilch, H. Cias, M. Sulowski, A. S. Wronski. Powder Metall., 46 (2003) 165.
12. G.F: Bocchini. Powder Metall. Progress, 4 (2004) 1.
13. S.C. Mitchell, A. Cias, Powder Metall. Progress, 4 (2004) 132.
14. H. Danninger, C. Gierl, S. Kremel, G. Leitner, K. Jaenicke-Roessler, Y. Yu. Powder Metall. Progress, 2 (2002) 125.
15. A. Salak, E. Dudrova. Kovove Materily, 11 (1973) 564.
16. T. Marcu, A. Molinari, G. Straffelini and S. Berg Powder Metall., 48 (2005) 139.
17. ASM Handbook, Vol.7, Powder Metal Technologies and Applications. "Consolidation Principles and Process Molding", pp.: 437-452.

***Садржај**: Челици високих перформанси (PM) се тренутно обрађују техником која се састоји од притискања праха који је атомизиран водом, затим синтеровањем и секундарним третманима и завршном обрадом. У овом раду проучени су синтеровани челици легирани хромом са два ниво легирања. Код челика легираних хромом површински оксид праха је од критичне важности за развој веза између честица током синтеровања. Редукција овог оксида првенствено зависи од три фактора: температура, тачка орошавања атмосфере и карботермичка редукција до које долази додатком графита. Трансформација почетне површине оксида се мења како се повећава температура током синтеровања у зависности од састава оксида. Карботермичка редукција би требала бити контрони механизам чак и кад се синтерује у атмосферема где има водоника. Ефекат карботермичке редукције се може посматрати проучавањем понашања узорака током проба кидања и проучавањем резултујућих ломљених површина.*

***Кључне речи**: синтеровани чеилици, хром, додирне површине током синтеровања, механичка својства.*